



Research Article

Enhanced photocatalysis, photoluminescence, and anti-bacterial activities of nanosize Ag: green synthesized via *Rauvolfia tetraphylla* (devil pepper)



S. P. Vinay¹ · Udayabhanu² · G. Nagarju² · C. P. Chandrappa³ · N. Chandrasekhar¹

© Springer Nature Switzerland AG 2019

Abstract

In the current study, we have built up a novel, green approach technique for the synthesis of silver nanoparticles (Ag NPs) from *Rauvolfia tetraphylla* leaves extract. The synthesized nanoparticles were thoroughly characterized using different analytical techniques like X-ray diffraction, Fourier transform infrared spectroscopy, UV–Vis spectroscopy (UV–Vis), scanning electron microscopy, energy-dispersive X-ray spectroscopy and transmission electron microscope analysis. It is confirmed as a cubic phase with average particle size about 40 nm with a spherical shape. Further, the characterized material was inspected for the photocatalytic degradation of most common environmental pollutants (carcinogenic organic dyes) like Methylene blue (M.B), Rhodamine B (Rh. B) and Rose bengal (R.B) with degradation efficiency of 81, 55 and 80% respectively. In addition, it was examined by optical property (photoluminescence) with blue emission by the excitation at 370 to 400 nm, which is useful for blue LEDs (light emitting diode). Furthermore, it also shows the superior anti-bacterial activity against gram-positive bacterias such as *Pseudomonas aeruginosa*, *Escherichia coli* and *Klebsiella aerogenes* and gram-negative bacteria *Staphylococcus aureus*. Ag NPs synthesized using *Rauvolfia tetraphylla* leaf extract exhibited a good photocatalytic and antibacterial activity. Hence, it's a first to report the synthesis of Ag NPs using natural reducing agent *Rauvolfia tetraphylla* leaf extract for Luminescence and Dye degradation applications.

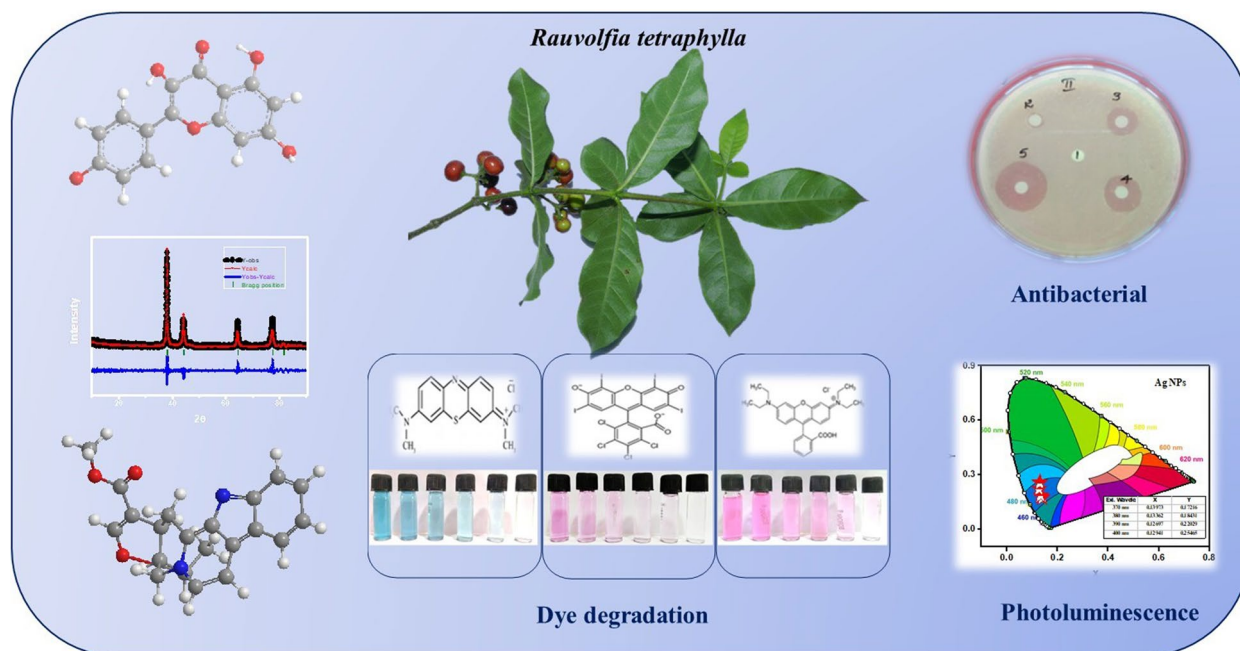
✉ N. Chandrasekhar, chandruharshu@gmail.com | ¹Research and Development Center, Department of Chemistry, Shridevi Institute of Engineering and Technology, Tumakuru 572106, India. ²Energy Materials Research Laboratory, Department of Chemistry, Siddaganga Institute of Technology, Tumakuru 572103, India. ³Department of Biotechnology, Shridevi Institute of Engineering and Technology, Tumakuru 572106, India.



SN Applied Sciences (2019) 1:477 | <https://doi.org/10.1007/s42452-019-0437-0>

Received: 28 February 2019 / Accepted: 1 April 2019 / Published online: 20 April 2019

Graphical abstract



Keywords Green synthesis · *Rauvolfia tetraphylla* · Photocatalyst · Dye degradation · Luminescence · Antibacterial

1 Introduction

In recent years, the improvement of efficient green chemistry methodology for synthesis of MNPs (metal nanoparticles) has attracted in the consideration of numerous researcher scholars. Continued work is being completed in order to discover eco-accommodating techniques for the creation of fine characterized NPs. Furthermore, the constraint to the utilization of these NPs is being addressed by a powerful novel method of generation that will create indistinguishable shape and size of NPs, and also particles with fractional or no poisonous quality to human wellbeing and the aerosphere. Dissimilar to chemically synthesized NPs, bio-synthesized MNPs depends on the green chemistry propose to authorize restricted presentation to the atmosphere and are relatively biocompatible. Green union involves numerous promising methodologies for the synthesis of MNPs with wanted properties [1]. Plant materials available in nature are widely used for green synthesis of metal nanoparticles. Till date, hundreds of plant extracts have been used in nanotechnological applications. The advancement in nanotechnology has come up with effective and nontoxic medication delivery mechanisms, less side effects, etc. [2, 3].

The term 'nano' initiates from the Greek word 'nanos' which means dwarf; and indicates a dimension on the

scale of 10^{-9} (one-billionth) of a meter in size [4]. There have been enormous advances in the field of nanotechnology, with numerous established methodologies to synthesize NPs with particular form and size. They have been computed for particular needs. Additionally, new applications for NPs and nanomaterials are growing extremely; while the acknowledgment of compelling nanomaterials has driven a massively enhanced appreciation of bioscience [5–11]. Numerous chemical and physical procedures are currently utilized to produce MNPs, which enable one to achieve particles with the chosen characteristics. In any case, these manufactured procedures are more expensive; works escalated and are possibly unsafe to the earth and living life forms [12, 13]. Accordingly, there is a conspicuous basic requirement for an option, financially savvy, safe and ecologically solid method for nanoparticle generation [14, 15]. Through the preceding examinations, it has been set up that numerous biological frameworks with green plants and green algae [16], yeast [17], bacteria [18], human cells [19], fungi [20], and diatoms [21] can change over inorganic metal ions into MNPs through the reductive capacities of the metabolites and proteins existing in these living beings.

Rauvolfia tetraphylla L. (Apocynaceae family) is a little, bush or tree that reaches six feet in stature. Plant leaves are spiral, average to shady green in color, arise in gatherings of four similarly sized leaves at every node and developed



Fig. 1 Photographic image of *Rauvolfia tetraphylla* plant

on a business (commercial) scale. *Rauvolfia tetraphylla* is a monetarily critical therapeutic plant due to the presence of numerous indole alkaloids in its individual parts [22]. In this report we are employing green method utilizing plant derived components for the green-synthesis of Ag nanoparticles using aquatic extract of *Rauvolfia tetraphylla* plant leaves as a fuel. The green-synthesized Ag NPs were characterized by X-ray diffraction (XRD), UV–Vis, Fourier transform infrared spectroscopy (FTIR), scanning electron microscopy (SEM), energy-dispersive X-ray spectroscopy (EDX) and transmission electron microscope (TEM) studies. Additionally, the green-synthesized Ag NPs were subjected for assessing the photoluminescence and photocatalytic properties.

2 Experimental

2.1 Materials used

All chemicals used were of analytical grade. AgNO_3 (Silver nitrate) was purchased from Merck, Mumbai, India. Rose bengal, Rhodamine B and Methylene blue dye were bought from S.D fine chemicals limited, Mumbai, India then utilized without further purification. *Rauvolfia tetraphylla* plant was collected from Devarayanadurga forest, Tumakuru, Karnataka, India.

2.2 Collection and preparation of leaves extract

The leaves of *Rauvolfia tetraphylla* (Fig. 1) plant was collected and washed methodically with tap water to

Table 1 Quantitative phytochemical constituent of *Rauvolfia tetraphylla*

S. no.	Phytochemicals constituent	Result
1	Alkaloids	+++
2	Flavonoids	++
3	Phenols	+
4	Tannins	+
5	Cardiac glycosides	+
6	Saponins	+
7	Antraquinones	–
8	Amino acids	+
9	Oxalate	–
10	Terpenoids	+

+++ , appreciable amount; ++, medium presence; +, presence in trace amount; –, negligible amount or completely absent

eliminate the dirt and dust particles and after that washed with distilled water. *Rauvolfia tetraphylla* leaves (20 g) were taken in 100 mL double distilled water and placed on heating mantle maintained at 60 °C for 20 min with stirring. Afterwards the mixture was cooled to ambient temperature, and then filtered through Whatman filter paper No.1. The resulting light green colored leaves extract was used as reducing and capping agent in green-synthesis method [23].

2.3 Phytochemical analysis

Rauvolfia tetraphylla leaves extract revealed the presence of bioactive secondary metabolites such as polyphenols in highly appreciable amount. Polyphenols contains more than 500 phytochemicals, which are normally happening micronutrients in plants. These classes of compounds act as great reducing agent during the green synthesis of NPs. The results of phytochemical screening of *Rauvolfia tetraphylla* leaves extract was subjected for the determination of polyphenol content, which revealed the presence of alkaloids in considerable amount. Also, our results clearly mention another important class of secondary metabolites of flavonoids, may also act as great source of reducing agents [24]. Some other phytochemicals constituent presence in minute or trace amounts; those are amino acids, terpenoids, flavonoids, tannins, phenols, saponins and cardiac glycosides (Table 1) [25]. These outcomes recommend that the *Rauvolfia tetraphylla* leaves extract is one of the best potential sources of bioactive secondary metabolites, which could effectively perform the role of reducing agents throughout the synthesis of Ag NPs.

2.4 Characterization techniques

Absorbance of Ag NPs were recorded using Agilent Technologies-Cary 60 UV-Vis spectrophotometer. X-ray diffraction (Rigaku Smart Lab) measurement was used to study the phase and purity of the sample. FTIR (BRUKER-ALPHA) was used to detect the possible functional groups of bio-molecules present in the compound. EDAX (OXFORD XMX N) determines the elemental analysis. Morphological distribution was examined using SEM (JEOL Model JSM-6390LV) and TEM (Jeol/JEM 2100). Photocatalytic dye degradation studies were carried out by Heber-Scientific Photoreactor. PL (Photoluminescence) studies were recored by Agilent technologies-Cary Eclipse Spectrofluorimeter.

2.5 Photocatalytic activity

The Photo-catalytic activity of the green synthesized Ag NPs were assessed by considering the dye degradation of Methylene blue (MB), Rhodamine B (Rh B) and Rose bengal (RB) in an aqueous solution at ambient temperature utilizing a 300 W visible light as radiance source. 20 mg of catalyst (Ag NPs) was mixed with 100 mL of 5 ppm Methylene blue, Rhodamine B and Rose bengal separately and solution was unceasingly stimulated in the dark chamber for about 30 min to attain adsorption-desorption equilibrium [26]. Further, the visible light was switched on. 2 mL of aliquot withdrawn for every 1 h interval. The samples were centrifuged using micro centrifuger for 10 min in order to segregate Ag NPs. Spectrophotometric evaluations were carried out by utilizing a quartz cell having a path length of 0.3 cm. Absorbance was recorded at a fixed wavelength using the UV-Vis spectrophotometer. The percentage degradation of the dye has been determined by the following equation.

$$\% \text{ of degradation} = (C_i - C_f) / C_i \times 100 \quad (1)$$

where C_i : initial concentrations of dye solution in ppm and C_f : final concentrations of dye solution in ppm respectively.

2.6 Detection of OH[•] radicals

OH[•] (Hydroxyl radicals) are the major reactive species in Photo-catalytic degradation reaction. The rate of development and identification of hydroxyl radicals throughout the degradation reaction can be estimated by a photoluminescence method using coumarin as an analysis molecule. In this procedure, 50 mg of Ag was dispersed in 100 mL of 0.5 mM aqueous coumarin solution in a glass jar. Coumarin solution was allowed for 10 min, past to

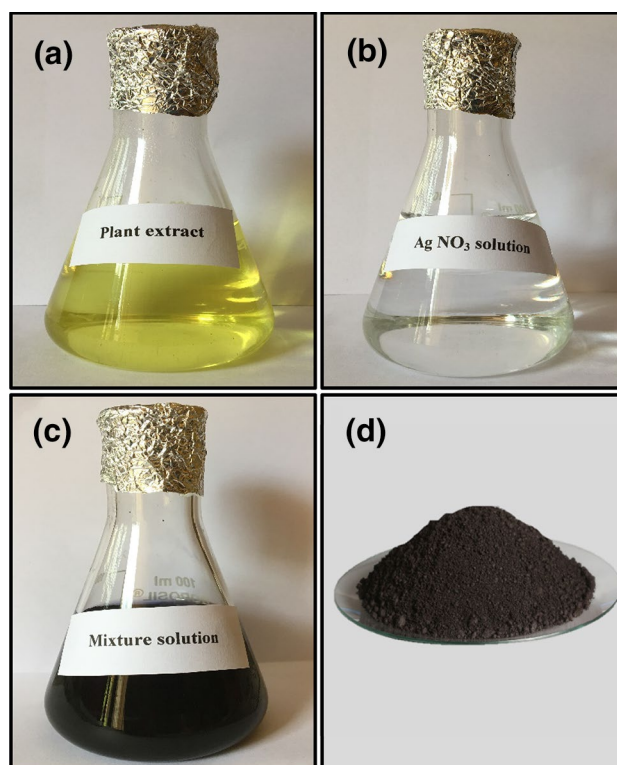


Fig. 2 a Plant extract, b AgNO₃ solution, c mixture solution, d Ag NPs

irradiation. This reaction was illuminated under the visible light of intensity 300 W/m² as a light source [27].

2.7 Synthesis of silver nanoparticles (Ag NPs)

The aqueous solution (5 mM) of silver nitrate (AgNO₃) were prepared and used for the synthesis of Ag NPs. The synthesis of Ag NPs was carried out at room temperature for 24 h and stored in dark to prevent agglomeration. *Rauvolfia tetraphylla* leaves extract (10 ml) was added to the AgNO₃ (90 ml) solution and placed on a magnetic stirrer for 10 min. The stirred mixture was allowed to undergo slow reduction into Ag NPs (Fig. 2) for 24 h to obtain complete bio-reduced silver ions. The obtained Ag NPs was purified by repeated centrifugation at 8000 rpm for 15 min using Remi Cooling centrifuge C-24. Further, the synthesized Ag NPs were dried and stored for further examination [28].

3 Results and discussion

The crystal size, structure, surface and applicability of the Ag NPs have been studied and examined in detail through different physicochemical methods like PXRD, UV-Vis, FTIR, SEM, EDAX, TEM and PL.

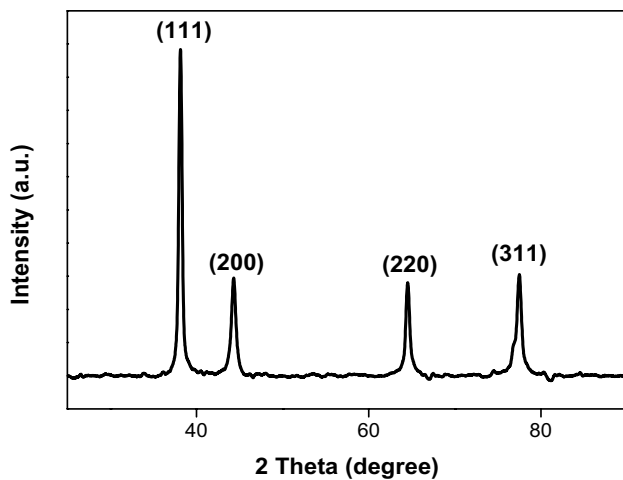


Fig. 3 PXRD pattern of the Ag NPs

3.1 Powder X-ray diffraction

Figure 3 shows the PXRD pattern, which is primary tool for the characterization of Ag NPs. The diffraction peaks at $2\theta = 38^\circ, 44^\circ, 64^\circ$ and 77° were indexed with the planes (111), (200), (220) and (311) for the resultant particles with cubic phase. The structure of obtained data well matches with the JCPDS card no. 1-1167 [29]. Plotted PXRD pattern indicates the formation high purity of the Ag NPs and there are no impurity peaks were observed. Further, using Debye–Scherrer’s equation, average crystallite size (D) was calculated [30]. This calculation reveals that the average crystallite size of Ag nanopowder was found to be 15.06 nm.

$$D = K\lambda/\beta \cos \theta \quad (2)$$

where K value 0.94, λ is wavelength, β is the full width at half maxima and D is the crystallite size.

Figure 4a shows the lattice parameter of Ag NPs synthesized by *Rauvolfia tetraphylla* leaves extract was

calculated by utilizing Rietveld refinement examination. The analysis was performed by utilizing the software FULLPROF assuming Fm-3m (225) space group for cubic type structure [31]. Pseudo-Voigt function was used in order to fit the few parameters to the data point: one scale factor, one zero shifting, four background, three cell parameters, five shape and width of the peaks, one global thermal factor and two asymmetric factors [27]. The Refined Parameters such as occupancy, atomic functional positions for Ag nanoparticles was summarized in Table 2. The diamond software was used for Rietveld refinement parameters the possible packing diagram which are shown in Fig. 4b. The fitting parameters: R_p , R_{wp} and χ^2 indicates a good agreement between the refined and observed PXRD patterns for the cubic Ag phase.

3.2 UV–Vis spectroscopy

Figure 5a shows the room temperature UV–vis spectrum of the Ag nanoparticles synthesized using *Rauvolfia tetraphylla* leaves extract. The maximum absorbance was obtained at 463 nm (confirming the formation of Ag nanoparticles) due to surface plasmon absorption. Past investigations recommended that a SPR peak located between 400 and 500 nm has been watched for Ag NPs and might be attributed to spherical structured nanoparticles [32]. A Figure 5b show the obtained band gap value was 2.74 eV; this value has been confirmed by indirect calculation from the absorption spectra using Tauc’s equation:

$$(\alpha h\nu)^2 = B(h\nu - E_{cb}) \quad (3)$$

where α is the absorption coefficient, $h\nu$ is the photon energy, E_{cb} is the conduction band energy, and B is a constant.

Fig. 4 a Rietveld refinement of Ag NPs, b packing diagram of Ag NPs

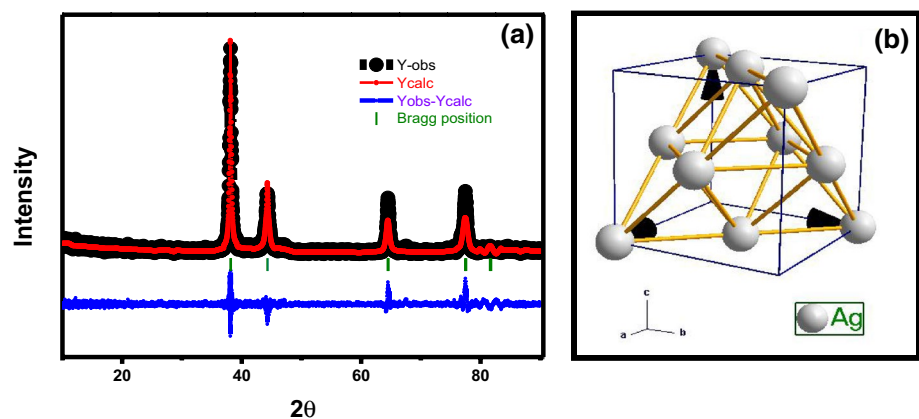


Table 2 Rietveld refined structural parameters for Ag NPs

Ag NPs	Ag (JCPDF No.:4-783)
Crystal system	Cubic
Space group	Fm-3m (225)
<i>Lattice parameters (Å°)</i>	
a=b=c	4.0866
$\alpha=\beta=\lambda$	90°
Unit cell volume (Å ³)	68.247
<i>Atomic coordinates</i>	
X	0.0000
Y	0.0000
z	0.0000
<i>Refinement parameters</i>	
R _p	20.5
R _{WP}	27.4
R _{Exp}	22.0
χ^2	1.55
GoF	1.2
R _{Bragg}	10.9
R _F	8.25
Density (g/cc ³)	10.498

Calculated band gap of Ag NPs is useful for the photocatalytic activity for the degradation of organic dyes [33, 34].

3.3 Fourier transform infrared spectroscopy

Figure 6 shows the FT-IR spectrum of the Ag NPs synthesized using *Rauvolfia tetraphylla* leaves extract. In this spectrum, a strong peaked at 3444 cm⁻¹ is attributed to stretching vibration of -OH, respectively, the peak at 1632 cm⁻¹ is associated with N-H bond and is assigned to amide-I bond of proteins presents in the extract [35]. The peaks at 1389 cm⁻¹ and 1123 cm⁻¹ are possibly the N-O symmetry stretching typical of the nitro compound

of leaves extract and C-N stretching of amines, respectively. The band at 1040 cm⁻¹ corresponds to C-F alkyl halide stretch vibration of proteins. These results recommended that the biological molecules conceivably perform twin function of synthesis and stabilization of Ag NPs [36].

3.4 Scanning electron microscopy

Figure 7a–c show the SEM images of Ag NPs examined using SEM analysis, the result exhibit morphology of Ag NPs and it evidently displays that particles are agglomerated crystals with almost uniform spherical shape [37].

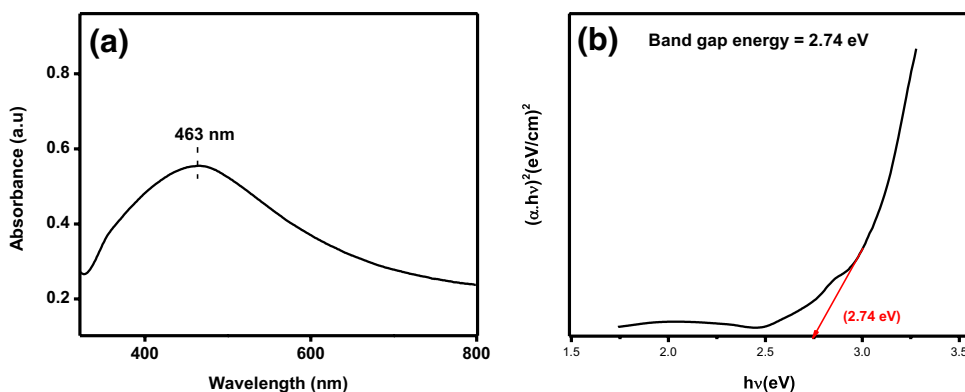
3.5 Energy-dispersive X-ray spectroscopy

Figure 8 shows the standard EDAX spectrum of Ag NPs, which describes the elemental analysis of the material. This shows a strong silver peaks together with weak carbon [38], oxygen, nitrogen and chlorine peaks, these peaks probably representing surface biomolecule capping structures originating from the *Rauvolfia tetraphylla* leaves extract [39].

3.6 Transmission electron microscope and selected area electron diffraction

Figure 9a shows the TEM image of Ag NPs, which are almost spherical in shape with average particle size of 40 nm (Fig. 9d). HRTEM image (Fig. 9b) of Ag NPs reveals that interplanar spacing of 0.14 nm corresponds to growing direction of Ag along (111) [40]. Selected area electron diffraction (SAED) pattern indicates the presence of (111), (200) and (220) planes in Ag NPs (Fig. 9c) are in consistent with the PXRD result (Fig. 3) [41].

Fig. 5 **a** UV-Vis spectrum of Ag NPs, **b** band gap energy of Ag NPs



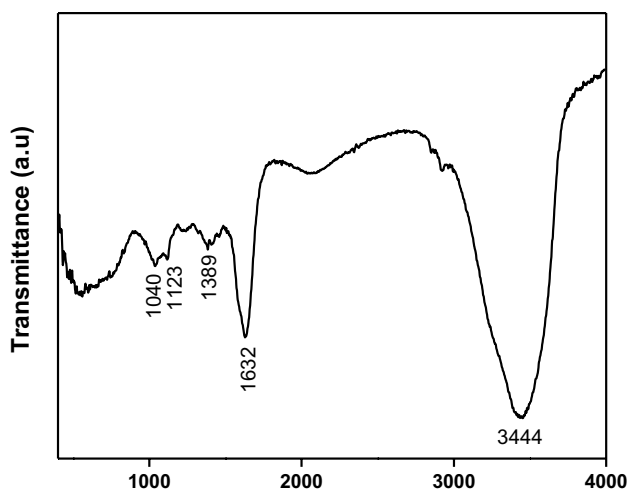


Fig. 6 FTIR spectrum of Ag NPs

3.7 Photocatalytic dye degradation

3.7.1 Degradation of Methylene blue

Methylene blue (MB) is a thiazine dye and it is known as methylthioninium chloride. The photocatalysis of

Methylene blue dye was carried using synthesized Ag NPs at varying time intervals in the visible region. Figure 10 shows that the rate of absorption band of Methylene blue from UV–Vis spectrophotometer at 663 nm. So, it is observed that the 5 ppm/100 mL of MB undergo 81% in a period of 5 h as shown in Fig. 14.

3.7.2 Degradation of Rhodamine B

Rhodamine B (Rh B) is a basic dye and it has two molecular forms of cationic and zwitterionic form. Cationic dyes are considered as toxic colorants and can cause harmful effects such as skin irritation, allergic dermatitis, cancer and mutations. Figure 11 shows the degradation of Rhodamine B using the UV–Vis spectrophotometer at 553 nm ($n \rightarrow \pi^*$ transition of C=N, C=O groups). So, it was observed that 5 ppm/100 mL of Rh B undergo degradation up to 55% in a period of 18 h (Fig. 14).

3.7.3 Degradation of Rose bengal

Rose bengal (RB) is a rose-colored anionic dye. Figure 12 shows the UV–Vis spectrum of Rose bengal. So, it was observed that 5 ppm/100 mL of RB dye degraded up to 80% with the expense of 4 h (Figs. 13, 14).

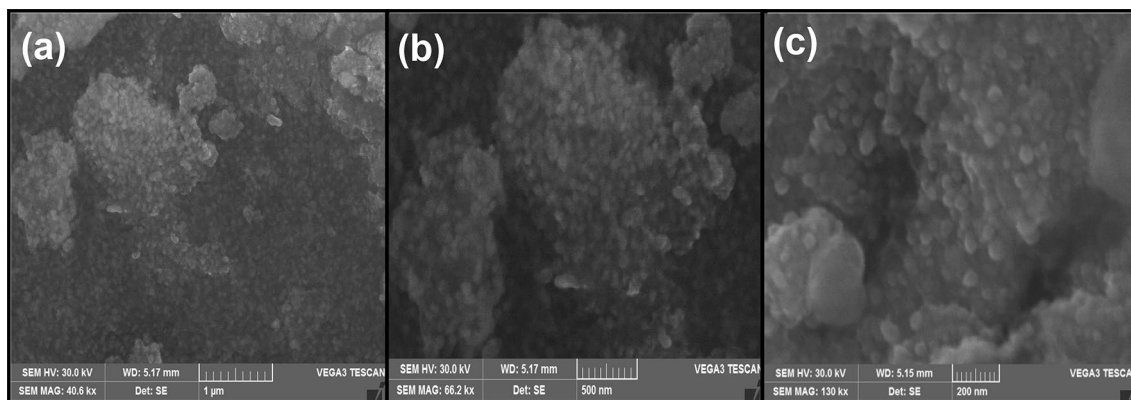


Fig. 7 a–c SEM images of Ag NPs

Fig. 8 EDX spectrum of synthesized Ag NPs

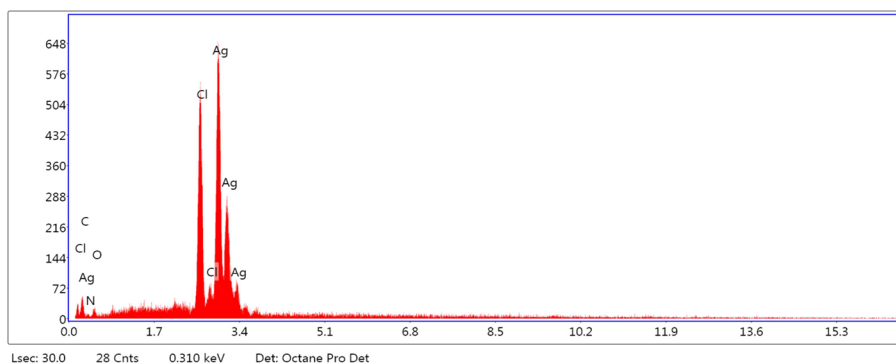


Fig. 9 **a** TEM image, **b** HR-TEM image, **c** SAED image, and **d** histogram show the range of particle size distribution

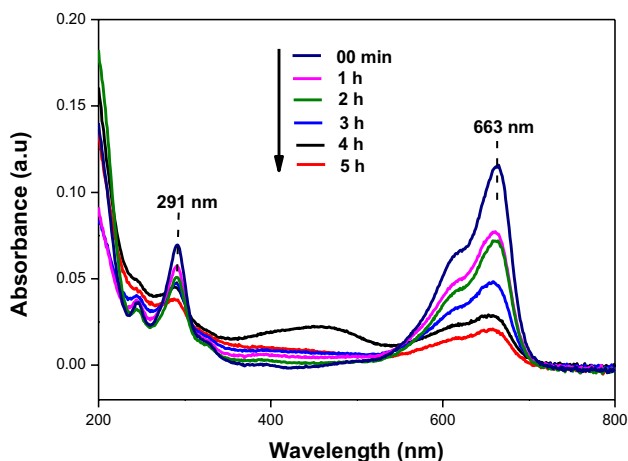
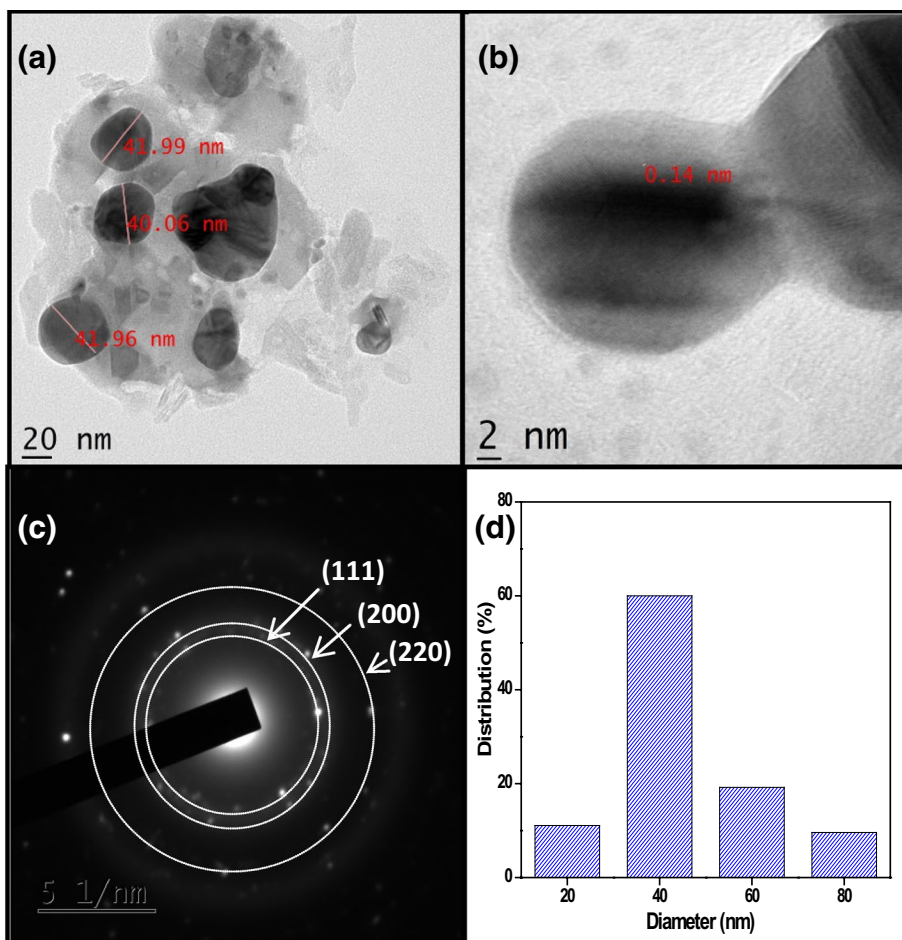


Fig. 10 Degradation of Methylene blue in the presence of synthesized Ag NPs

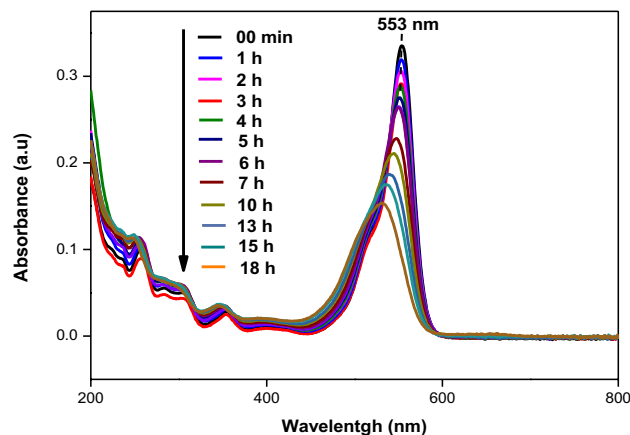


Fig. 11 Degradation of Rhodamine B in the presence of synthesized Ag NPs

3.8 Catalyst recycling

To assess the stability of the photocatalyst, recycled experiments for the photocatalyst was tested again MB, Rh B and RB dyes. These experiments were carried out with 20 mg

of catalyst with 100 mL of 5 ppm dye for 4 h. The degradation efficiency of MB, Rh B and RB were almost the same for 6 cycles. Figure 15 clearly represents that RB degrades nearly 81%, MB degrades almost 77% and Rh B degrades closely

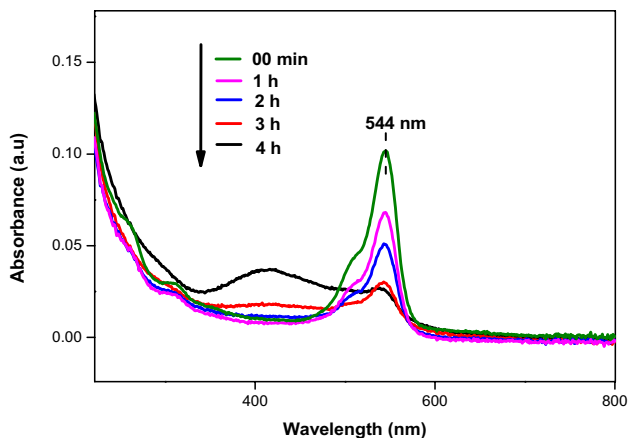
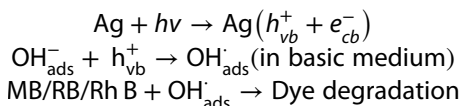


Fig. 12 Degradation of Rose bengal in the presence of synthesized Ag NPs

17% efficiencies for all six cycles. The efficiency of degradation is due to stable spherical shaped Ag NPs.

3.9 Mechanism

Photocatalytic dye degradation of MB, Rh B and RB dye in the presence of Ag NPs is shown in the three steps reaction mechanism (Scheme 1).



3.10 Detection of OH[·] radicals

Figure 16 shows that Hydroxyl radicals respond with Coumarin at 460 nm with exceedingly formed fluorescent compound (7-hydroxyl Coumarin) [43]. It clearly indicates

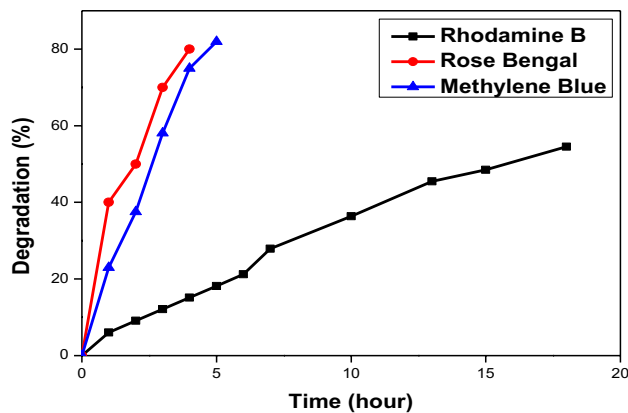


Fig. 14 Percentage degradation of visible light in presence of synthesized Ag NPs

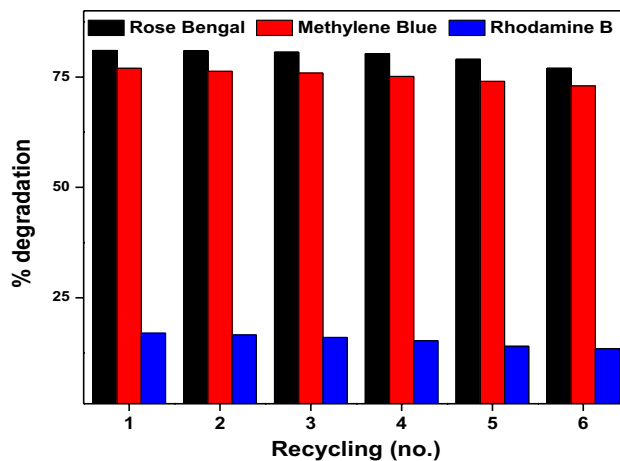


Fig. 15 Recycling of 20 mg catalyst for the degradation of 100 mL of 5 ppm dyes concentration for 4 h

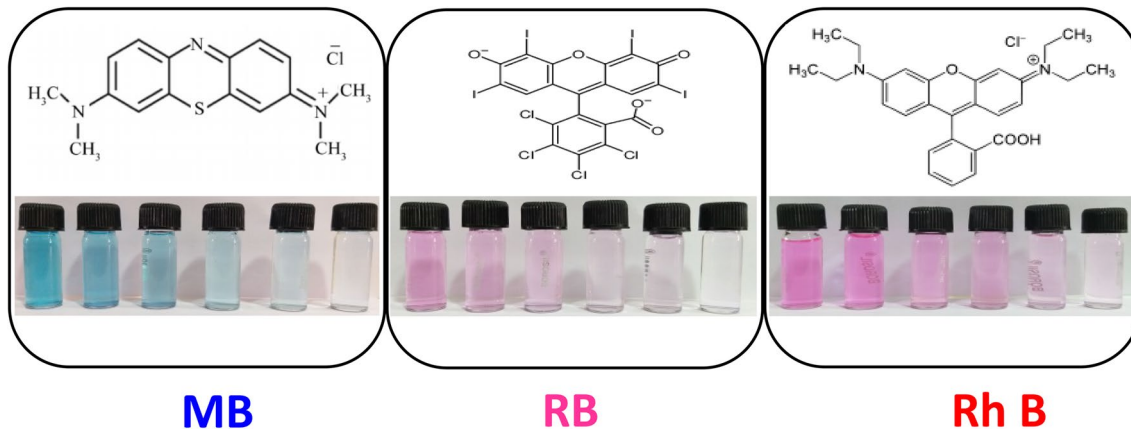


Fig. 13 Structure and colour of organic dyes Methylene blue (MB), Rose bengal (RB) and Rhodamine B (Rh B)

Scheme 1 Schematic mechanism for the dye degradation

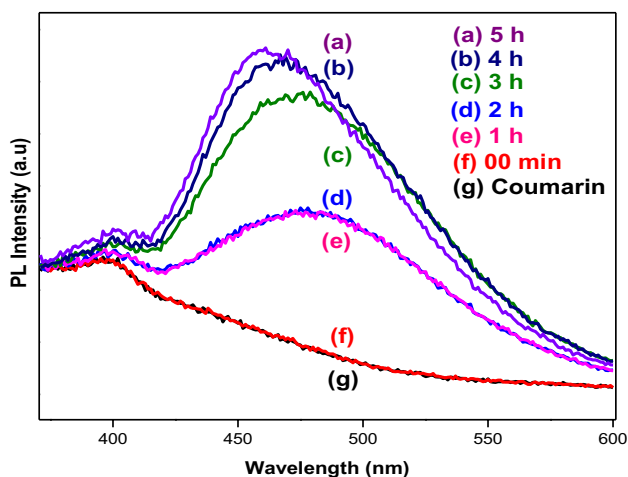
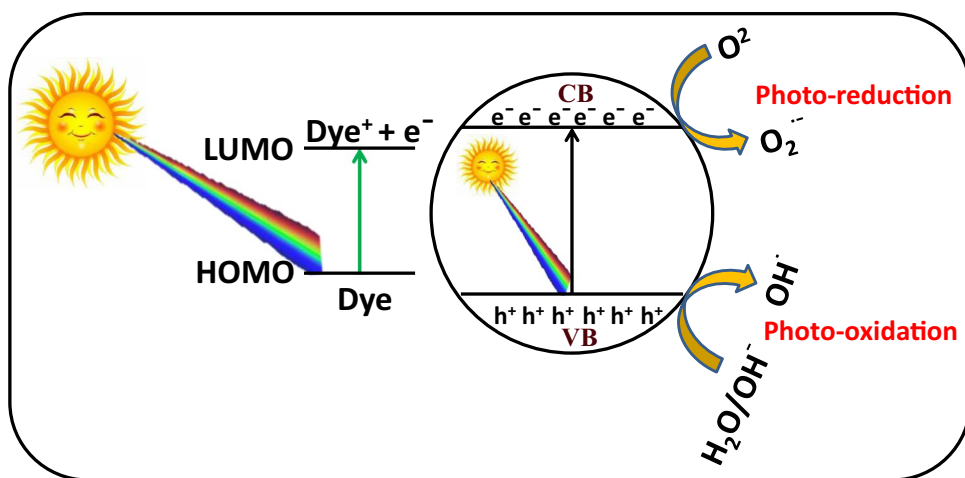


Fig. 16 PL spectra of Coumarin solution against hydroxyl radicals

that, these Hydroxyl radicals (OH) are responsible for the photocatalytic degradation of MB, Rh B and RB dyes.

3.11 Photoluminescence (PL) studies

The photoluminescence of noble metals could be viewed as an excitation of electrons from occupied *d* bands into states above the fermi level. Subsequent electron-phonon and hole-phonon scattering processes led to energy loss and finally photoluminescent recombination of an electron from an occupied *sp* band with the hole. Figure 17 shows the photoluminescence spectrum of Ag NPs recorded at room temperature. In Fig. 17a show that excitation spectrum of Ag NPs, which has shown the strong excitation peak at 390 nm with the emission wavelength 484 nm. Figure 17b reveals the emission spectrum of Ag NPs with the excitation wavelengths

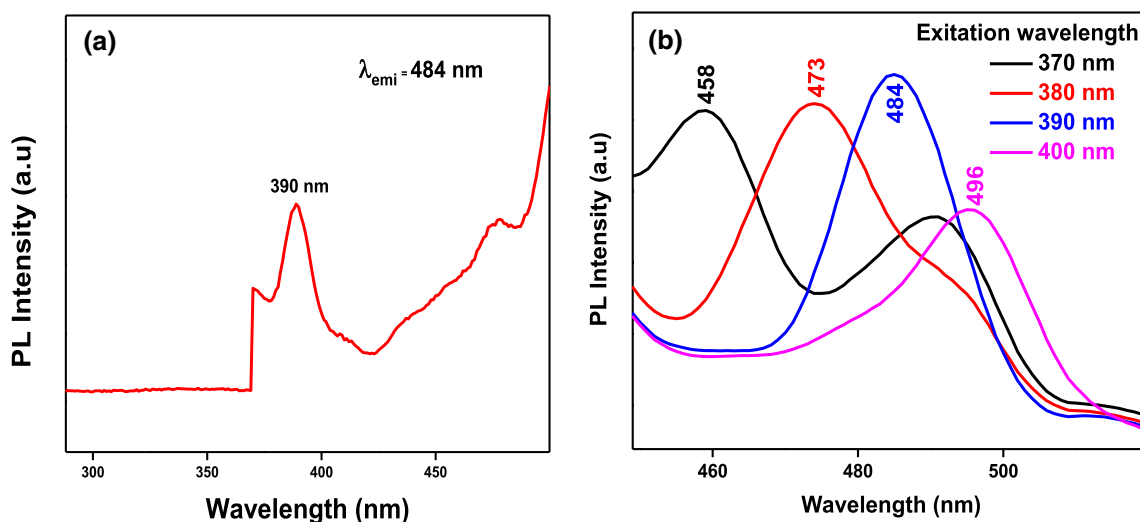


Fig. 17 **a** Photoluminescence excitation spectrum of Ag NPs: emission centred at 390 nm and **b** Emission spectrum of Ag NPs: excited at 370, 380, 390 and 400 nm

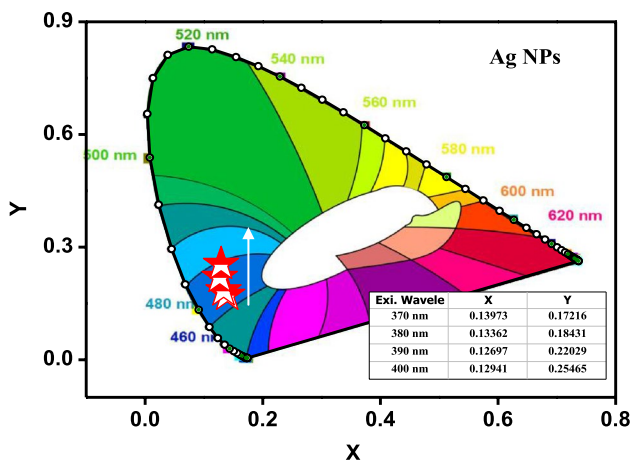


Fig. 18 CIE diagram for Ag NPs

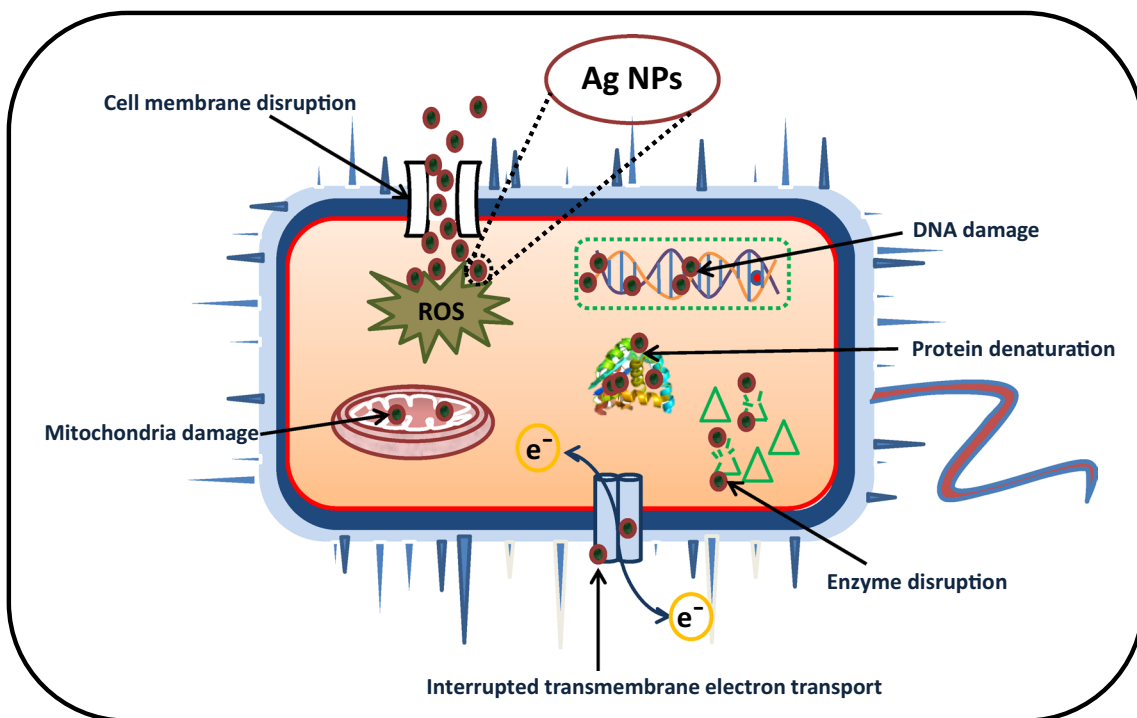
of 370, 380, 390 and 400 nm and obtained the emission peaks at 458, 473, 484 and 496 nm, respectively. As the excitation wavelength increases, the emission peaks were red shifted towards the higher wavelength with slightly more intensity. Upon increase in excitation wavelength of Ag NPs, the two peaks obtained for the excitation at 370 nm was gradually merge at 484 nm and form a single peak [44].

The purity in color of any photoluminescent material was expressed in terms of chromaticity coordinates. For Ag NPs, it was calculated from the emission spectrum

using the CIE (Commission International De l'Eclairage) system. The CIE chromaticity diagram of Ag NPs under excitations at 370, 380, 390 and 400 nm was shown in Fig. 17b. The corresponding CIE colour coordinates (x and y) obtained were given in inset of Fig. 18. It is cleared from the CIE diagram that pure Ag NPs emits broad blue light, which is the average of all the emission peaks. As the excitation increases, the colour chromaticity shifted towards green edge in CIE diagram, this is due to the emission peaks shifted towards higher wavelength [45].

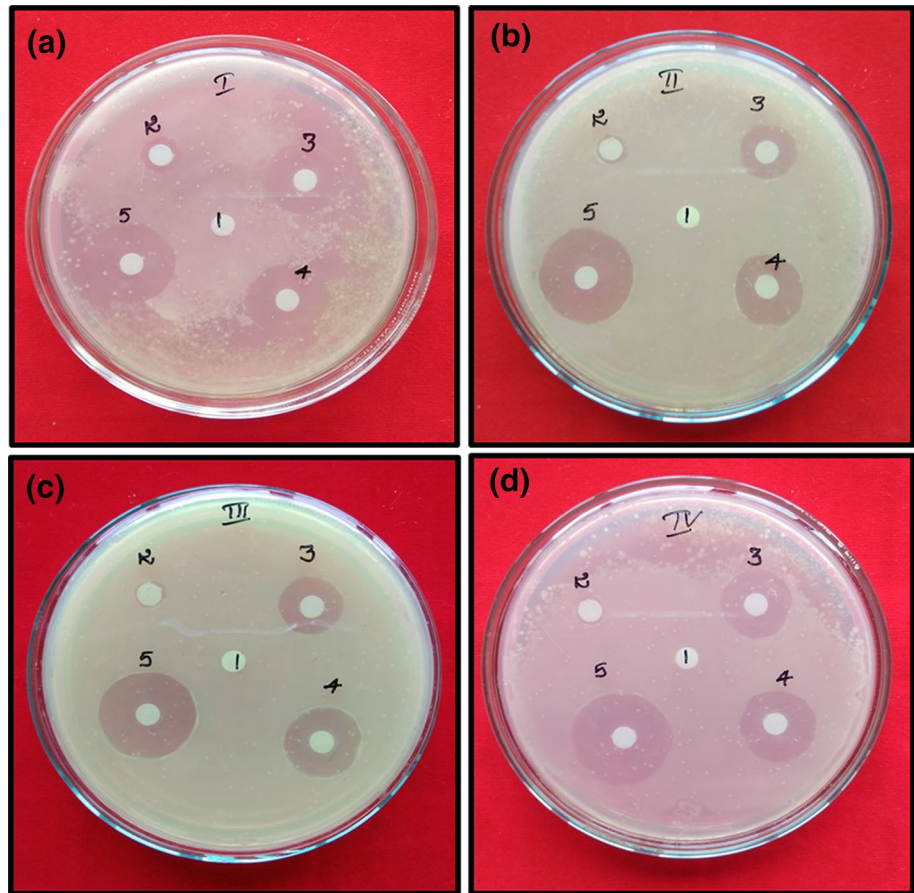
3.12 Antibacterial assay

The mechanism of antibacterial activity of Ag NPs has been testified by numerous researchers, the cell death and leakage of cell membrane is because of the discharge of Ag^+ ion and generation of reactive oxygen species (singlet oxygen, superoxide anion radical, hydroxyl radical and hydrogen peroxide) the smaller size particles gives a more reactive surface zone to interact with the bacteria enhancing a superior anti-bacterial ability. Production of the reactive oxygen species on the surface of the Ag nanoparticles when the light causes oxidative stress in the bacterial cell wall, eventually leading to the death of the cells. Ag with a positive charge and cell membrane with negative charge mutually attract.



Scheme 2 Mechanism of antibacterial activity

Fig. 19 Zone of inhibition of **a** *Escherichia coli*, **b** *Pseudomonas aeruginosa*, **c** *Klebsiella aerogenes* and, **d** *Staphylococcus aureus* in presence of Ag NPs synthesized using leaves extract of *Rauvolfia tetraphylla*



Notes: (1) Control, (2) Plant extract, (3) Ag NPs (500 µg/µL), (4) Ag NPs (1000 µg/µL), (5) Standard.

Table 3 Antibacterial activity of Ag NPs on pathogenic bacterial strains

S. no.	Treatment	<i>Escherichia coli</i> (mean ± SE)	<i>Pseudomonas aeruginosa</i> (mean ± SE)	<i>Klebsiella aerogenes</i> (mean ± SE)	<i>Staphylococcus aureus</i> (mean ± SE)
1	Control	NA	NA	NA	NA
2	Plant extract	2.19 ± 0.33*	1.41 ± 0.31*	0.92 ± 0.42*	0.87 ± 0.33*
3	Ag NPs (500 µg/µL)	7.00 ± 0.00	5.23 ± 0.33*	5.53 ± 0.31*	6.75 ± 0.33*
4	Ag NPs (1000 µg/µL)	7.51 ± 0.43*	6.24 ± 0.33*	6.37 ± 0.17*	7.00 ± 0.00
5	Standard	9.30 ± 0.54*	11.16 ± 0.33*	11.33 ± 0.12*	11.15 ± 0.37*

Values are the mean ± SE of inhibition zone in mm

NA symbols represent no antibacterial activity was found in this work

* $P < 0.01$ as compared with the control group

Further, Ag⁺ enters into the cell membrane and reacts with the thiol groups present on the cell membrane and destruction it leading to the death of the cells. Considering the above facts, the possible schematic diagram is shown in Scheme 2 [46].

The significant antibacterial properties of Ag NPs were assessed by taking Gram positive *Staphylococcus aureus*

and Gram-negative *Pseudomonas aeruginosa*, *Klebsiella aerogenes* and *E-coli* bacteria by disc diffusion method [47]. In disc diffusion method, the Ag nanoparticles shows significant anti-bacterial action on all the 4 bacterial strains (Fig. 19). The measured zone of inhibition was mentioned in Table 3.

4 Conclusion

The present work illustrates a facile green method for the synthesis of Ag NPs using aqueous *Rauvolfia tetraphylla* leaves extract. Further, this method offers numerous advantages like cost effective, low temperature, non-toxic, eco-friendly, simple, quick and the effortlessness for the synthesis. The phyto-components effectively act as reducing agents and lead to the synthesis of Ag NPs. PXRD pattern shows that the Ag NPs are cubic phase structure, with an average crystallite size (D) of 15.06 nm. DRS spectrum show the band gap value was 2.74 eV for green synthesized Ag NPs. TEM image confirms the formation of Ag NPs with almost spherical in shape. These nanoparticles show more stability and virtuous Photocatalytic activity toward the photodegradation of Methylene blue (MB), Rhodamine B (Rh B) and Rose bengal (RB). The photo-luminescence band in the visible luminescence range resulting from the higher surface interstitial defects reduces the electrons/holes recombination and consequently increases the photocatalytic activity. Finally, the green synthesized Ag nanoparticles exhibit significant bactericidal activity against *S. aureus*, *E. coli*, *K. aerogenes* and *P. aeruginosa* using the disc diffusion method. In summary, the study fruitfully proves that facile green-synthesis of multifunctional Ag NPs was achieved by naturally occurring plant parts.

Acknowledgements Dr. Chandrasekhar and Vinay thank Dr. M. R. Hulinaykar, Managing Trustee, Sri Shridevi Charitable Trust, and Shridevi Institute of Engineering and Technology for encouragement and support for research work. The authors also thank Siddaganga Institute of Technology for providing the lab facilities. Udayabhanu thanks to CSIR, New Delhi, for Senior Research Fellowship {09/1204(0001)/2018-EMR-1}. Dr. G. N. Thanks DST Nanomission (SR/NM/NS-1262/2013) for financial support.

Compliance with ethical standards

Conflict of interest The authors declare that they have no conflict of interest.

References

- Nishanthi R, Malathi S, Palani P (2019) Green synthesis and characterization of bioinspired silver, gold and platinum nanoparticles and evaluation of their synergistic antibacterial activity after combining with different classes of antibiotics. *Mater Sci Eng, C* 96:693–707
- Chandrasekhar N, Vinay SP (2017) Yellow colored blooms of *Argemone mexicana* and *Turnera ulmifolia* mediated synthesis of silver nanoparticles and study of their antibacterial and antioxidant activity. *Applied Nanoscience* 7:851–861
- Vinay SP, Chandrasekhar N (2017) Characterization and Green Synthesis of Silver Nanoparticles from Plumeria Leaves Extracts: study of Their Antibacterial Activity. *IOSR-JAC* 10:57–63
- Narayanan KB, Sakthivel N (2010) Biological synthesis of metal nanoparticles by microbes. *Adv Colloid Interface Sci* 156:1–13
- Taylor E, Webster TJ (2011) Reducing infections through nanotechnology and nanoparticles. *Int J Nanomed* 6:1463
- Goudarzi Mojgan, Mir Noshin, Mousavi-Kamazani Mehdi, Bagheri Samira, Salavati-Niasari Masoud (2016) Biosynthesis and characterization of silver nanoparticles prepared from two novel natural precursors by facile thermal decomposition methods. *Scientific Reports* 6(1):32539
- MojganGoudarzi MasoudSalavati-Niasari, FatemehYazdian MahnazAmiri (2019) Sonochemical assisted thermal decomposition method for green synthesis of $\text{CuCo}_2\text{O}_4/\text{CuO}$ ceramic nanocomposite using *Dactylopius Coccus* for anti-tumor investigations. *J Alloy Compd* 788:944–953
- Goudarzi M, Salavati-Niasari M, Amiri M (2019) Effective induction of death in breast cancer cells with magnetite $\text{NiCo}_2\text{O}_4/\text{NiO}$ nanocomposite. *Compos Part B Eng* 166:457–463
- Mohandes F, Salavati-Niasari M (2014) Freeze-drying synthesis, characterization and *in vitro* bioactivity of chitosan/graphene oxide/hydroxyapatite nanocomposite. *RSC Adv* 4:25993–26001
- Vinay SP, Chandrashekar N, Chandrappa CP (2017) Biosynthesis of silver nanoparticles using leaves extracts of *Acalypha hispida* burm.f. and study of their antibacterial activity. *Int Res J Nat Appl Sci* 4(7):9–19
- Mahnaz Amiri, Masoud Salavati-Niasari, Ahmad Akbari (2017) A magnetic $\text{CoFe}_2\text{O}_4/\text{SiO}_2$ nanocomposite fabricated by the sol-gel method for electrocatalytic oxidation and determination of L-cysteine. *Microchim Acta* 184:825–833
- Tsuji M, Miyamae N, Lim S, Kimura K, Zhang X, Hikino S, Nishio M (2006) Crystal structures and growth mechanisms of Au@Ag core-shell nanoparticles prepared by the microwave-polyol method. *Cryst Growth Des* 6:1801–1807
- Gan PP, Li SFY (2012) Potential of plant as a biological factory to synthesize gold and silver nanoparticles and their applications. *Rev Environ Sci Bio* 11:169–206
- Sharma HS, Ali SF, Hussain SM, Schlager JJ, Sharma A (2009) Influence of engineered nanoparticles from metals on the blood-brain barrier permeability, cerebral blood flow, brain edema and neurotoxicity. An experimental study in the rat and mice using biochemical and morphological approaches. *J Nano Sci Nanotech* 9:5055–5072
- Porel S, Singh S, Harsha SS, Rao DN, Radhakrishnan T (2005) Nanoparticle embedded polymer: in situ synthesis, free-standing films with highly monodisperse silver nanoparticles and optical limiting. *Chem Mater* 17:9–12
- Govindaraju K, Basha SK, Kumar VG, Singaravelu G (2008) Silver, gold and bimetallic nanoparticles production using single-cell protein (*Spirulina platensis*) Geitler. *J Mater Sci* 43:5115–5122
- Kowshik M, Deshmukh N, Vogel W, Urban J, Kulkarni SK, Paknikar K (2002) Microbial synthesis of semiconductor CdS nanoparticles, their characterization, and their use in the fabrication of an ideal diode. *Biotechnol Bioeng* 78:583–588
- Lengke MF, Fleet ME, Southam G (2007) Biosynthesis of silver nanoparticles by filamentous cyanobacteria from a silver (I) nitrate complex. *Langmuir* 23:2694–2699
- Anshup Venkataraman JS, Subramaniam C, Kumar RR, Priya S, Kumar TS, Omkumar R, John A, Pradeep T (2005) Growth of gold nanoparticles in human cells. *Langmuir* 21:11562–11567
- Rautaray D, Ahmad A, Sastry M (2003) Biosynthesis of CaCO_3 crystals of complex morphology using a fungus and an actinomycete. *J Amer Chem Soc* 125:14656–14657
- Scarano G, Morelli E (2002) Characterization of cadmium- and lead-phytochelatin complexes formed in a marine microalga in response to metal exposure. *Biometals* 15:145–151

22. Amjad Ali M, Iqbal Firoz A, Khan Kalam, Khan Mohib (2013) Ethno-Phyto-Pharmacological Overview on *Rauwolfia tetraphylla* L. *Int J Pharm Phytopharmacol. Res* 2(4):247–251
23. Kalaiarasi R, Prasannaraja G, Venkatachalama P (2013) A rapid biological synthesis of silver nanoparticles using leaf broth of *Rauwolfia tetraphylla* and their promising antibacterial. *Indo Am J Pharm Res* 3(10):8052–8062
24. Nair Vadakkemuriyil Divya, Panneerselvam Rajaram, Gopi Ragupathi (2012) Studies on methanolic extract of *Rauwolfia* species from Southern Western Ghats of India—In vitro antioxidant properties, characterisation of nutrients and phytochemicals. *Ind Crops Prod* 39:17–25
25. Nandhini VS, Vijistella Bai G (2014) Screening of phyto-chemical constituents, trace metal concentrations and antimicrobial efficiency of *Rauwolfia tetraphylla*. *IJPBS* 4(1):47–52
26. Suresh D, Udayabhanu, Nethravathi PC, Lingaraju K, Rajanaika H, Sharma SC, Nagabhushana H (2015) ECG assisted green synthesis of ZnO nanopowders: photodegradative, antimicrobial and antioxidant activities. *Spectrochim Acta Part A Mol Biomol Spectrosc* 136:1467–1474
27. Udayabhanu, Nagaraju G, Nagabhushana H, Basavaraj RB, Raghu GK, Suresh D, Rajanaika H, Sharma SC (2016) Green, nonchemical route for the synthesis of ZnO superstructures, Evaluation of its applications towards Photocatalysis. *Photoluminescence and Bio-sensing. Cryst Growth Des* 16(12):6828–6840
28. Vinay SP, Chandrashekar N, Chandrappa CP (2017) Eco-friendly approach for the green synthesis of silver nanoparticles using flower extracts of *Sphagneticola trilobata* and study of antibacterial activity. *International Journal of Pharmacy and Biological Sciences (IJPBS)* 7(2):145–152
29. Wang Hongqiang, Jia Lichao, Li Liang, Li Xiangyou, Warkocka Zaneta Swiatkowska, Kawaguchi Kenji, Pyatenko Alexander, Koshizaki Naoto (2013) Photomediated assembly of single crystalline silver spherical particles with enhanced electrochemical performance. *J Mater Chem A* 1:692–698
30. Vinay SP, Chandrashekar N, Chandrappa CP (2017) One-step green synthesis of silver nanoparticles using flower extract of *Tabebuia argentea* Bur & K. Sch. and their antibacterial activity. *Res J Pharm Biol Chem Sci (RJPBCS)* 8(4):527–534
31. Madan HR, Sharma SC, Udayabhanu, Suresh D, Vidya YS, Nagabhushana H, Rajanaik H, Anantharaju KS, Prashantha SC, Sadananda Maiya P (2015) Facile Green Fabrication of Nanostructure ZnO Plates, Bullets, Flower, Prismatic tip, Closed pine cone: their Antibacterial, Antioxidant, Photoluminescent and Photocatalytic Properties. *Spectrochim Acta Part A Mol Biomol Spectrosc* 152:404–416
32. Hamad Abubaker, Li Lin, Liu Zhu, Zhong Xiang Li, Liu Hong, Wang Tao (2015) Generation of Silver Titania Nanoparticles from Ag-Ti alloy via Picosecond Laser Ablation and their Antibacterial Activities. *RSC Advances* 5(89):72981–72994
33. Gharibshahi Leila, Saion Elias, Gharibshahi Elham, Shaari Abdul Halim, Matori Khamirul Amin (2017) Structural and Optical Properties of Ag Nanoparticles Synthesized by Thermal Treatment Method. *Materials* 10:402
34. Aziz A, Khalid M, Saeed Akhtar M, Nadeem M, Gilani ZA, Huda UI, Asghar HMN, Rehman J, Ullah Z, Saleem M (2018) Structural, morphological and optical investigations of silver nanoparticles synthesized by sol-gel auto combustion method. *Digest Journal of Nanomaterials and Biostructures* 13(3):679–683
35. Prakash P, Gnanaprakasam P, Emmanuel R, Arokiyaraj S, Saravanan M (2013) Green synthesis of silver nanoparticles from leaf extract of *Mimusops elengi*, Linn. for enhanced antibacterial activity against multi drug resistant clinical isolates. *Colloids Surf B* 108:255–259
36. Jyoti Kumari, Singh Ajeet (2016) Green synthesis of nanostructured silver particles and their catalytic application in dye degradation. *Journal of Genetic Engineering and Biotechnology* 14:311–317
37. Sood Richa, Chopra Dimple Serhi (2018) Optimization of reaction condition to fabricate *Ocimum sanctum* synthesized silver nanoparticles and its application to nano gel systems for burn wounds. *Mater Sci Eng, C* 92:575–589
38. Wang Lu, Yanan Wu, Xie Jia, Sheng Wu, Zhenqiang Wu (2018) Characterization, antioxidant and antimicrobial activities of green synthesized silver nanoparticles from *Psidium guajava* L. leaf aqueous extracts. *Mater Sci Eng, C* 86:1–8
39. Moodley Jerushka S, Krishna Suresh Babu Naidu, Pillay Karen, Sershen Patrick Govender (2018) Green synthesis of silver nanoparticles from *Moringa oleifera* leaf extracts and its antimicrobial potential. *Adv Nat Sci Nanosci Nanotechnol* 9:015011
40. Nagaraju G, Udayabhanu, Shivaraj, Prashanth SA, Shastri M, Yathish KV, Anupama C, Rangappa D (2017) Electrochemical heavy metal detection, Photocatalytic, Photoluminescence, Biodiesel production and Antibacterial activities of Ag-ZnO nanomaterial. *Mater Res Bull* 94:54–63
41. Nam Sunghyun, Park Bosoon, Brian D (2018) Condon, Water-based binary polyol process for the controllable synthesis of silver nanoparticles inhibiting human and foodborne pathogenic bacteria. *RSC Adv* 8:21937–21947
42. Udayabhanu, Nethravathi PC, Pavan Kumar MA, Suresh D, Lingaraju K, Rajanaika H, Nagabhushana H, Sharma SC (2015) *Tinospora cordifolia* mediated facile green synthesis of cupric oxide nanoparticles and their photocatalytic, antioxidant and antibacterial properties. *Mater Sci Semicond Process* 33:81–88. <https://doi.org/10.1016/j.mssp.2015.01.034>
43. Suresh D, Nethravathi PC, Udayabhanu, Rajanaika H, Nagabhushana H, Sharma SC (2015) Green synthesis of multifunctional zinc oxide (ZnO) nanoparticles using *Cassia fistula* plant extract and their photodegradative, antioxidant and antibacterial activities. *Mater Sci Semicond Process* 31:446–454
44. Ping He, Xing-Hai Shen, Hong-Cheng Gao (2004) Photoluminescence Phenomenon during the Formation of Silver Nanoparticles. *Acta Phys Chim Sin* 20(10):1200–1203
45. Stael C, Cruz R, Naranjo B, Debut A, Angulo Y (2018) Improvement of cochineal extract (*Dactylopius coccus* Costa) properties based on the green synthesis of silver nanoparticles for application in organic devices. *J Nanotechnol.* <https://doi.org/10.1155/2018/3751419>
46. Madhukara Naik M, Bhojya Naik HS, Nagaraju G, Vinuth M, Vinu K, Rashmi SK (2018) Effect of aluminium doping on structural, optical, photocatalytic and antibacterial activity on nickel ferrite nanoparticles by sol-gel auto-combustion method. *J Mater Sci: Mater Electron* 29(23):20395–20414
47. He Huawei, Tao Gang, Wang Yejing, Cai Rui, Guo Pengchao, Chen Liqun, Zuo Hua, Zhao Ping, Xia Qingyou (2017) In situ green synthesis and characterization of sericin-silver nanoparticle composite with effective antibacterial activity and good biocompatibility. *Mater Sci Eng, C* 80:509–516
48. Suresh D, Nethravathi PC, Udayabhanu Nagabhushana H, Sharma SC (2015) Spinach assisted green reduction of graphene oxide and its antioxidant and dye absorption properties. *Ceram Int* 41:4810–4813

Publisher's Note Springer Nature remains neutral with regard to jurisdictional claims in published maps and institutional affiliations.